

Chapter 26

Models for Precession Electron Diffraction

Laurence D. Marks

Abstract Precession Electron Diffraction has become an increasingly popular method of obtaining crystallographic data, and may well replace older methods such as selected area diffraction or microdiffraction. While a full model has to involve a dynamical calculation, some approximations give some indication how the results vary as a function of thickness and precession angle. This note reviews some of the basic models, their advantages and failures as well as some of the open issues.

26.1 Introduction

Over the last few years Precession Electron Diffraction (PED), a technique for acquiring electron diffraction intensities, invented in 1994 by Vincent and Midgley [1] has started to emerge as a viable technique for determining structures based solely upon the intensities, and/or with some assistance from crystallographic phases determined using HREM or similar techniques. An incomplete list of references is [1–50]. It was clear from the first attempts to use the method coupled with direct methods that it gave remarkably better results than conventional diffraction techniques except in relatively special cases such as surfaces where the diffraction intensities are very close to kinematical. Hence the quandary; electron diffraction can only be properly be described using dynamical diffraction, but tools based upon a kinematical formulation work. Why? While the detailed answer to this is still not fully understood, many of the details are and I will here briefly describe the main models along with their advantages and limitations.

L.D. Marks (✉)

Department of Materials Science and Engineering, Northwestern University,
Evanston, IL 60201, USA
e-mail: l-marks@northwestern.edu

26.2 Kinematical Model

The kinematical model has to be mentioned as it is the simplest. The result one gets is that the intensities are proportional to the square of the crystallographic structure factor. Unfortunately except for special cases such as surfaces or graphene monolayers the method has only a very limited relevance for standard samples as an accurate model, as illustrated in Fig. 26.1, failing by 10 nm thickness.

26.3 Blackman Model

The Blackman model [51, 52] makes the assumption that the integration over angles can be considered as equivalent to a complete integration of a two-beam diffraction problem for all possible angles. In more detail, the intensity for a given reflection can be written as the integral of a Bessel function:

$$I(t) = \int_0^{A_g} J_0(2x) dx \quad A_g = \frac{\pi t}{\xi_g^2}$$

Where ξ_g is the standard extinction distance which scales inversely with the structure factor and t is the thickness. The result one obtains is that the intensity, for a relatively thick crystal, scales directly as the crystallographic structure factor; for a thin crystal it scales as the square of the structure factors. While this is again a useful, simple approximation which has been sometimes used and is better than kinematical, there are several fundamental problems with it:

- It neglects most dynamical diffraction effects, as the two-beam model really only applies for specific orientations.
- It neglects the fact that in a precession experiment only a limited range of angles are used.

Unfortunately it is not accurate, $R1 > 40\%$ for 200 \AA , see Fig. 26.2.

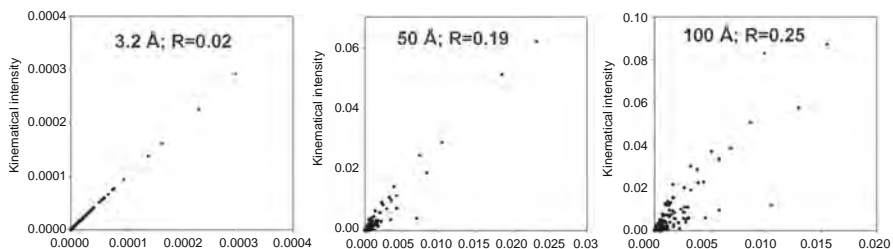


Fig. 26.1 Comparison of kinematical intensities (y axis) versus full dynamical calculations (x axis) for different thicknesses for $(\text{Ga,In})_2\text{SnO}_4$ with the $R1$ shown

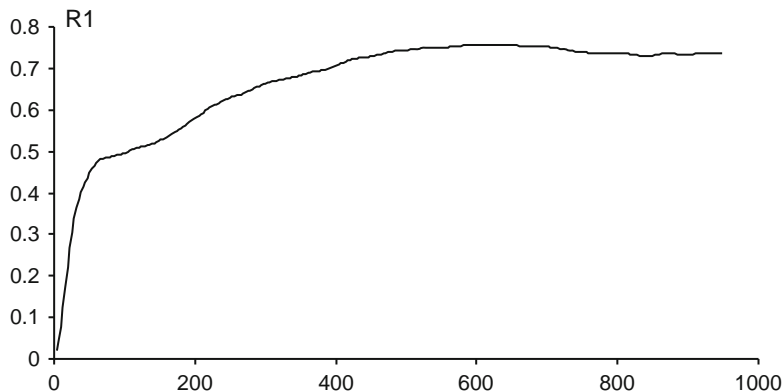


Fig. 26.2 Values of the R1 from a Blackman model versus a full dynamical calculation (y-axis) for $(\text{Ga,In})_2\text{SnO}_4$ as a function of thickness in Angstroms along the x-axis

26.4 Methods Based Upon Lorentz-Type Corrections

From the earliest days of PED a different approach has been to try and separate the contributions associated with the integration over angle and dynamical diffraction effects, what has been called a Lorentz correction. In more formal fashion, the intensity would be written as

$$I(g) = L(g) * B(g)$$

where $L(g)$ is an approximate form to take into account the integration range, and $B(g)$ is purely a diffraction term, for instance Kinematical or the Blackman equation. The concept is that one might then be able to precalculate $L(g)$ and remove it, thereby obtaining a better form. A simple form for $L(g)$ suggested by Gjønnes [2] is

$$L(g) = g \sqrt{1 - \left(\frac{g}{2R_0}\right)^2}$$

Where R_0 is the precession scan angle in reciprocal Angstroms. While this is an interesting idea unfortunately to date it has not been particularly successful as illustrated in Fig. 26.3.

26.5 1s Channeling Model

The concept of a channeling approach is to expand the electron wave in terms of local orbitals rather than plane waves, e.g. [53–56]. One can then approximate by using just the 1s states, which works well for HREM and STEM imaging [57].

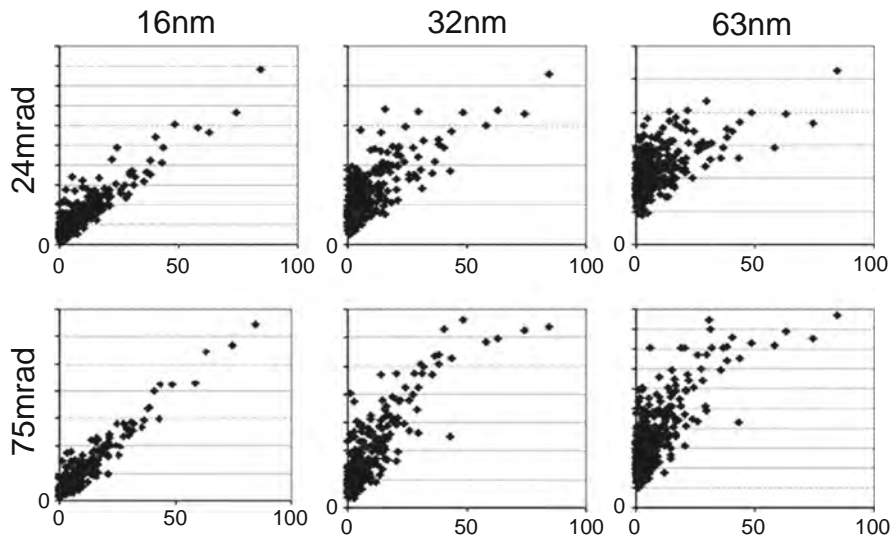


Fig. 26.3 Scatter plot of Lorentz-corrected data (y-axis) versus the true values (x-axis) for $(\text{Ga}, \text{In})_2\text{SnO}_4$ with two different precession angles and three different thicknesses

At least in order of simplicity, this model is an attractive approach. The result of the model is “atom-like” features and it has been shown that even though the results are dynamical, the deviations from kinematical are in fact statistical in character rather than being systematic [58, 59]. Since both direct methods and refinements are (in principle) stable against statistically random deviations, it is therefore true that in some cases on a zone axis these methods will work well. Alas, while there may be some relationship to what one finds in a PED pattern, to date this approach has not proved to be useful. (A 1s-model leads to scattering which is dominated by atomic strings which is similar to what PED yields so there may be some connection, but so far there is no proof beyond qualitative intuition.)

26.6 Two-Beam Model

The first model to account for at least some of the effects present is a two-beam model with a proper tracking of the range of integration. A specific form [26] is

$$C_{2beam}(g, t, \phi) = F_g^2 \left(\frac{1}{\xi_g^2} \int_0^{2\pi} \frac{\sin^2(\pi t s_{eff})}{(s_{eff})^2} d\theta \right)^{-1}$$

Where the effective excitation error $s_{eff} = (s^2 + \xi_g^2)^{1/2}$ is used. This is better, but again not perfect and breaks down for a thickness much beyond 10 nm as illustrated in Fig. 26.4.

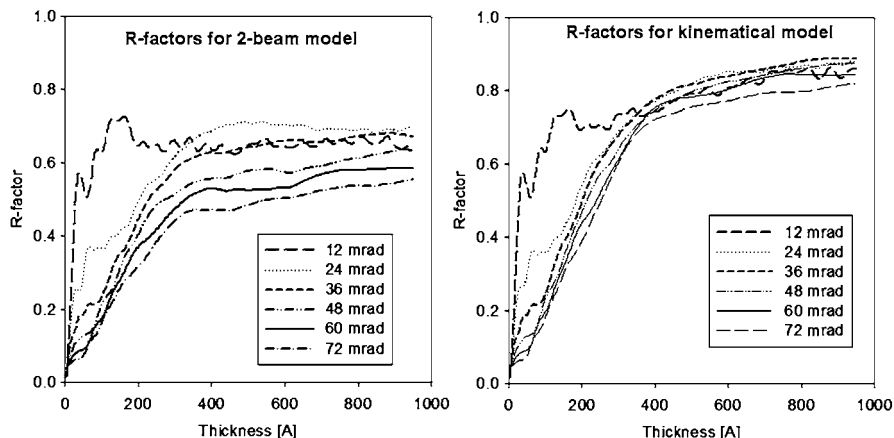


Fig. 26.4 Comparison for $(\text{Ga,In})_2\text{SnO}_4$ of the R1 for a two-beam model versus thicknesses (*left*) compared to a kinematical model (*right*). Unfortunately while there is some improvement, it is not enough

26.7 Full Multislice or Bloch Wave Methods

Good agreement between experimental and calculated intensities has been obtained using methods where all the dynamical diffraction effects (except fine details of inelastic scattering/adsorption) are taken into account. These are based upon either the multislice method [60–63], a fast numerical integration of the intensities, or Bloch Wave methods [64–66] where a matrix problem is solved. Assuming that the potential used is the same for the two methods, it is known that they give identical results provided that they have been properly coded.

The approach [13], as illustrated in Fig. 26.5 is to consider all different incident beam directions and integrate the final intensity over these, for instance the set 1–8 below.

Without any additional refinement one can easily obtain an R1 of about 0.1, as illustrated below in Figs. 26.6 and 26.7.

26.8 Intensity Ordering

An explanation of why the methods work, which unfortunately slightly begs the question of the details of when they will fail, is intensity ordering [67]. Instead of the intensities being simply related to the structure factors as in kinematical or Blackman approaches, the hypothesis of this model is that reflections with large structure factors lead to large intensities in PED, those with small structure factors small intensities. By inspection this is largely true for the plots shown above which

Fig. 26.5 Schematic of a dynamical simulation. For a range of different tilts a full calculation is performed and the results are summed. Specific results for eight illustrative tilts are shown; in general 512–1,024 different values are used

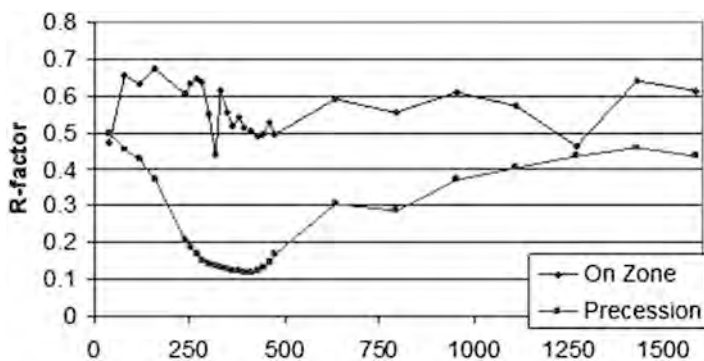
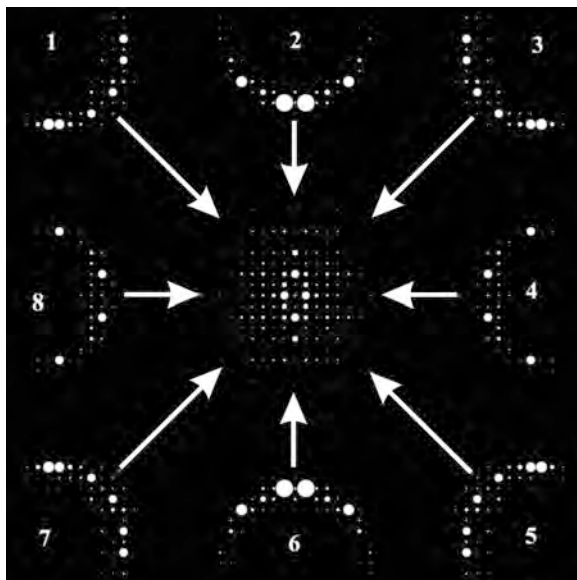


Fig. 26.6 R1 as a function of thickness in Angstroms from a multislice calculation using experimental data for $(\text{Ga,In})_2\text{SnO}_4$ both on-zone (*upper line*) and precessed (*lower line*). The minimum with precessed data is much clearer, and the R1 much lower

plot the kinematical structure factors versus the true values. This is a sufficient condition for direct methods to work, indeed in the early days of the technique with “by eye” measurement of intensities for x-ray diffraction from film, structures were solved by dividing the intensities into those which were strong, those which were of medium intensity and the weak ones. Classical direct methods only use the strong intensities, so provided that these are representative then Σ_2 and similar relationships will be preserved.

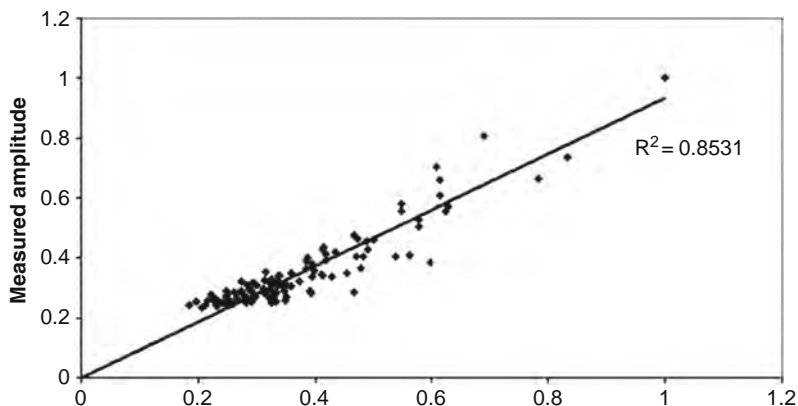


Fig. 26.7 Plot of measured amplitudes versus multislice calculations for the optimum thickness shown in Fig. 26.6

26.9 Summary

For certain PED has emerged as a powerful tool for solving structures. The intensities are much better behaved than those from zone-axis diffraction particularly if larger tilt angles are used. Unfortunately most simple models to date fail to explain fully the dynamical diffraction effects in enough detail so one has to do a full calculation.

Fortunately the PED intensities are not chaotic, but are ordered which is enough for direct methods to work and there is now extensive empirical evidence showing that this approach can be used to obtain an initial structure for later refinement either (or both) from powder x-ray data or by using a dynamical approach.

What remains as a problem is how to refine the structure, or perform structure completion – in most respects the later is a more significant issue as structure completion is in many respects why direct methods work. The large $R1$ values with kinematical models are problematic. In principle one might be able to use a two-beam model as an improvement upon kinematical in a refinement as implied by an initial estimate [26] and one can use it to approximately invert a set of intensity data. This might be a viable refinement approach as it would be faster than a full dynamical method, and this is currently under investigation.

There are also other alternatives. For instance, some time ago it was suggested by Peng [68] that one could use a quasi-kinematical approach, an idea that may well be worth returning to. Alternatively there are ways to exploit the implicit periodicity in reciprocal space (Brillouin Zone folding) so rather than calculating 1,024 different tilts a much smaller number of Bloch wave calculations is needed, perhaps only 1 if chosen judiciously or at most 8 [47]. This could give a 10^3 improvement in speed and might make a Bloch wave refinement viable on a reasonable computer; full

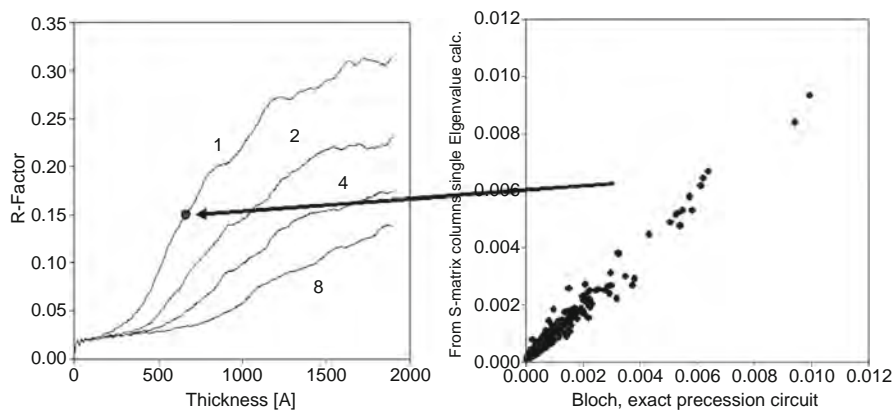


Fig. 26.8 Plot the R1 for $(\text{Ga,In})_2\text{SnO}_4$ using a limited number of tilts exploiting Brillouin-Zone folding for different thicknesses relative to a full calculation (*left*) with a scatter plot of the intensities on the *right* for one Bloch-wave as *arrowed*

refinements will be unrealistically slow if all points are used. This is illustrated in Fig. 26.8 below which compares the results of an accurate Bloch wave calculation with 1,024 tilts to a much smaller set.

Despite these limitations, PED has moved from the early days when it was a curiosity to a mainstream tool for electron microscopists to use to determine structures where real-space imaging methods are problematic, for instance when there is beam damage or ambiguities in the interpretation of the images. Even with its current limitations the R1 values obtained are in most cases rather better than one can obtain with alternative approaches.

References

1. Vincent R, Midgley PA (1994) Double conical beam-rocking system for measurement of integrated electron diffraction intensities. *Ultramicroscopy* 53:271–282
2. Gjonnes K (1997) On the integration of electron diffraction intensities in the Vincent-Midgley precession technique. *Ultramicroscopy* 69:1–11
3. Berg BS, Hansen V, Midgley PA, Gjonnes J (1998) Measurement of three-dimensional intensity data in electron diffraction by the precession technique. *Ultramicroscopy* 74:147–157
4. Gjonnes J, Hansen V, Berg BS, Runde P, Cheng YF, Gjonnes K, Dorset DL, Gilmore CJ (1998) Structure model for the phase Al_mFe derived from three-dimensional electron diffraction intensity data collected by a precession technique. Comparison with convergent-beam diffraction. *Acta Crystallogr Sect A* 54:306–319
5. Gjonnes K, Cheng YF, Berg BS, Hansen V (1998) Corrections for multiple scattering in integrated electron diffraction intensities. Application to determination of structure factors in the [001] projection of Al_mFe . *Acta Crystallogr Sect A* 54:102–119
6. Midgley PA, Sleight ME, Saunders M, Vincent R (1998) Measurement of Debye-Waller factors by electron precession. *Ultramicroscopy* 75:61–67

7. Gemmi M, Zou X, Hovmöller S, Migliori A, Vennström M, Andersson Y (2002) Structure of Ti_2P solved by three-dimensional electron diffraction data collected with the precession technique and high-resolution electron microscopy. *Acta Crystallogr Sect A* 59:117–126
8. Gjonnes J, Hansen V, Kverneland A (2004) The precession technique in electron diffraction and its application to structure determination of nano-size precipitates in alloys. *Microsc Microanal* 10:16–20
9. Own CS (2005) System design and verification of the precession electron diffraction technique. Northwestern, Evanston
10. Own CS, Marks LD, Sinkler W (2005) Electron precession: a guide for implementation. *Rev Sci Instrum* 76:1866612
11. Kverneland A, Hansen V, Vincent R, Gjonnes K, Gjonnes J (2006) Structure analysis of embedded nano-sized particles by precession electron diffraction. η' -precipitate in an Al-Zn-Mg alloy as example. *Ultramicroscopy* 106:492–502
12. Own CS, Marks LD, Sinkler W (2006) Precession electron diffraction I: multislice simulation. *Acta Crystallogr Sect A* 62:434–443
13. Own CS, Sinkler W, Marks LD (2006) Rapid structure determination of a metal oxide from pseudo-kinematical electron diffraction data. *Ultramicroscopy* 106:114–122
14. Weirich TE, Portillo J, Cox G, Hibst H, Nicolopoulos S (2006) Ab initio determination of the framework structure of the heavy-metal oxide $CsxNb_{2.54}W_{2.46}O_{14}$ from 100 kV precession electron diffraction data. *Ultramicroscopy* 106:164–175
15. Boulahya K, Ruiz-Gonzalez L, Parras M, Gonzalez-Calbet JM, Nickolsky MS, Nicolopoulos S (2007) Ab initio determination of heavy oxide perovskite related structures from precession electron diffraction data. *Ultramicroscopy* 107:445–452
16. Avilov A, Kuligin K, Nicolopoulos S, Nickolskiy MS, Boulahya K, Portillo J, Lepeshov G, Sobolev B, Collette JP, Martin N, Robins AC, Fischione P (2007) Precession technique and electron diffractometry as new tools for crystal structure analysis and chemical bonding determination. *Ultramicroscopy* 107:431–444
17. Dudka AP, Avilov AS, Nicolopoulos S (2007) Crystal structure refinement using Bloch-wave method for precession electron diffraction. *Ultramicroscopy* 107:474–482
18. Gemmi M, Nicolopoulos S (2007) Structure solution with three-dimensional sets of precessed electron diffraction intensities. *Ultramicroscopy* 107:483–494
19. Morniroli JP, Redjaimia A (2007) Electron precession microdiffraction as a useful tool for the identification of the space group. *J Microsc-Oxf* 227:157–171
20. Morniroli JP, Redjaimia A, Nicolopoulos S (2007) Contribution of electron precession to the identification of the space group from microdiffraction patterns. *Ultramicroscopy* 107:514–522
21. Nicolopoulos S, Morniroli JP, Gemmi M (2007) From powder diffraction to structure resolution of nanocrystals by precession electron diffraction. *Z Kristallogr* 26:183–188
22. Oleynikov P, Hovmoller S, Zou XD (2007) Precession electron diffraction: observed and calculated intensities. *Ultramicroscopy* 107:523–533
23. Own CS, Dellby N, Krivanek OL, Marks LD, Murfitt M (2007) Aberration-corrected precession electron diffraction. *Microsc Microanal* 13:96–97
24. Own CS, Sinkler W, Marks LD (2007) Prospects for aberration corrected electron precession. *Ultramicroscopy* 107:534–542
25. Sinkler W, Own CS, Ciston J, Marks LD (2007) Statistical treatment of precession electron diffraction data with principal components analysis. *Microsc Microanal* 13:954–955
26. Sinkler W, Own CS, Marks LD (2007) Application of a 2-beam model for improving the structure factors from precession electron diffraction intensities. *Ultramicroscopy* 107:543–550
27. Ciston J, Deng B, Marks LD, Own CS, Sinkler W (2008) A quantitative analysis of the cone-angle dependence in precession electron diffraction. *Ultramicroscopy* 108:514–522
28. Ciston J, Own CS, Marks LD (2008) Cone-angle dependence of ab-initio structure solutions using precession electron diffraction. *Electron Microsc Multiscale Model* 999:53–65
29. Morniroli JP, Auchterlonie GJ, Drennan J, Zou J (2008) Contribution of electron precession to the study of perovskites displaying small symmetry departures from the ideal cubic ABO_3 perovskite: applications to the $LaGaO_3$ and LSGM perovskites. *J Microsc-Oxf* 232:7–26

30. Morniroli JP, Houdellier F, Roucau C, Puiggali J, Gestì S, Redjaimia A (2008) LACDIF, a new electron diffraction technique obtained with the LACBED configuration and a Cs-corrector: comparison with electron precession. *Ultramicroscopy* 108:100–115
31. Rauch EF, Veron M, Portillo J, Bultreys D, Maniette Y, Nicolopoulos S (2008) Automatic crystal orientation and phase mapping in TEM by precession diffraction. *Microsc Anal Nanotechnol Suppl* 22:S5–S8
32. Xie D, Baerlocher C, McCusker LB (2008) Combining precession electron diffraction data with X-ray powder diffraction data to facilitate structure solution. *J Appl Crystallogr* 41:1115–1121
33. Boullay P, Dorcet V, Perez O, Grygiel C, Prellier W, Mercey B, Hervieu M (2009) Structure determination of a brownmillerite $\text{Ca}_2\text{Co}_2\text{O}_5$ thin film by precession electron diffraction. *Phys Rev B* 79:184108
34. Jacob D, Cordier P, Morniroli JP, Schertl HP (2009) Application of precession electron diffraction to the characterization of (021) twinning in pseudo-hexagonal coesite. *Am Mineral* 94:684–692
35. Ji G, Morniroli JP, Auchterlonie GJ, Drennan J, Jacob D (2009) An efficient approach to characterize pseudo-merohedral twins by precession electron diffraction: application to the LaGaO_3 perovskite. *Ultramicroscopy* 109:1282–1294
36. Morniroli JP, Ji G (2009) Identification of the kinematical forbidden reflections from precession electron diffraction. In: Moeck P, Hovmoller S, Nicolopoulos S, Rouvimov S, Petkov V, Gateshki M, Fraundorf P (eds) *Electron crystallography for materials research and quantitative characterization of nanostructured materials*. Materials Research Society, Warrendale
37. Mugnaioli E, Gorelik T, Kolb U (2009) “Ab initio” structure solution from electron diffraction data obtained by a combination of automated diffraction tomography and precession technique. *Ultramicroscopy* 109:758–765
38. Barnard JS, Eggeman AS, Sharp J, White TA, Midgley PA (2010) Dislocation electron tomography and precession electron diffraction – minimising the effects of dynamical interactions in real and reciprocal space. *Philos Mag* 90:4711–4730
39. Cascarano GL, Giacomazzo C, Carrozzini B (2010) Crystal structure solution via precession electron diffraction data: the BEA algorithm. *Ultramicroscopy* 111:56–61
40. Eggeman AS, White TA, Midgley PA (2010) Is precession electron diffraction kinematical? Part II A practical method to determine the optimum precession angle. *Ultramicroscopy* 110:771–777
41. Gemmi M, Klein H, Rageau A, Strobel P, Le Cras F (2010) Structure solution of the new titanate $\text{Li}_4\text{Ti}_8\text{Ni}_3\text{O}_{21}$ using precession electron diffraction. *Acta Crystallogr Sect B* 66:60–68
42. Hadermann J, Abakumov AM, Tsirlin AA, Filonenko VP, Gonnissen J, Tan HY, Verbeeck J, Gemmi M, Antipov EV, Rosner H (2010) Direct space structure solution from precession electron diffraction data: resolving heavy and light scatterers in $\text{Pb}_{13}\text{Mn}_9\text{O}_{25}$. *Ultramicroscopy* 110:881–890
43. Jacob D, Cordier P (2010) A precession electron diffraction study of α , β phases and Dauphine twin in quartz. *Ultramicroscopy* 110:1166–1177
44. Ji G, Jacob D, Morniroli JP (2010) The state of order in Fe-Al studied by precession electron diffraction. *Philos Mag Lett* 91:54–60
45. Moeck P, Rouvimov S (2010) Precession electron diffraction and its advantages for structural fingerprinting in the transmission electron microscope. *Z Kristallogr* 225:110–124
46. Rauch EF, Portillo J, Nicolopoulos S, Bultreys D, Rouvimov S, Moeck P (2010) Automated nanocrystal orientation and phase mapping in the transmission electron microscope on the basis of precession electron diffraction. *Z Kristallogr* 225:103–109
47. Sinkler W, Marks LD (2010) Characteristics of precession electron diffraction intensities from dynamical simulations. *Z Kristallogr* 225:47–55
48. White TA, Eggeman AS, Midgley PA (2010) Is precession electron diffraction kinematical? Part I: “Phase-scrambling” multislice simulations. *Ultramicroscopy* 110:763–770
49. Zhang DL, Gruner D, Oleynikov P, Wan W, Hovmoller S, Zou XD (2010) Precession electron diffraction using a digital sampling method. *Ultramicroscopy* 111:47–55

50. Klein H, David J (2011) The quality of precession electron diffraction data is higher than necessary for structure solution of unknown crystalline phases. *Acta Crystallogr Sect A* 67:297–302
51. Blackman M (1939) On the intensities of electron diffraction rings. *Proc R Soc A* 173:68–82
52. Gjønnnes K, Cheng YF, Berg BS, Hansen V (1998) Corrections for multiple scattering in integrated electron diffraction intensities. Application to determination of structure factors in the [001] projection of Al_mFe . *Acta Crystallogr Sect A* 54:102–119
53. Lindhard J (1964) Motion of swift charged particles, as influenced by strings of atoms in crystals. *Phys Lett* 12:126–128
54. Gemmell DS (1974) Channelling and related effects in the motion of charged particles through crystals. *Rev Mod Phys* 46:129–227
55. Kambe K, Lehmppfuhl G, Fujimoto F (1974) Interpretation of electron channeling by the dynamical theory of electron diffraction. *Z Naturforsch* 29:1034–1044
56. Tamura A, Ohtsuki YH (1974) Quantum mechanical study of rosette motion channeling. *Phys Status Solidi B* 62:477–480
57. Geuens P, Van Dyck D (2002) The S-state model: a work horse for HRTEM. *Ultramicroscopy* 93:179–198
58. Hu JJ, Chukhovskii FN, Marks LD (2000) Statistical dynamical direct methods I. The effective kinematical approximation. *Acta Crystallogr Sect A* 56:458–469
59. Chukhovskii FN, Hu JJ, Marks LD (2001) Statistical dynamical direct methods II. The three-phase structure invariant. *Acta Crystallogr Sect A* 57:231–239
60. Cowley JM, Moodie AF (1957) The scattering of electrons by atoms and crystals I. A new theoretical approach. *Acta Crystallogr* 10:609–619
61. O’Keefe M (1973) n-Beam lattice images IV. Computed two-dimensional images. *Acta Crystallogr Sect A* 29:389–401
62. Ishizuka K (1982) Multislice formula for inclined illumination. *Acta Crystallogr Sect A* 38:773–779
63. Ishizuka K (2004) FFT multislice method – the silver anniversary. *Microsc Microanal* 10:34–40
64. Humphreys CJ (1979) The scattering of fast electrons by crystals. *Rep Prog Phys* 42:1825–1887
65. Spence JCH, Zuo JM (1992) *Electron microdiffraction*. Plenum Press, New York
66. Allen LJ, Josefsson TW, Leeb H (1998) Obtaining the crystal potential by inversion from electron scattering intensities. *Acta Crystallogr Sect A* 54:388–398
67. Marks LD, Sinkler W (2003) Sufficient conditions for direct methods with swift electrons. *Microsc Microanal* 9:399–410
68. Peng L-M (2000) Quasi-dynamical electron diffraction – a kinematic type of expression for the dynamical diffracted-beam amplitudes. *Acta Crystallogr Sect A* 56:511–518